J BONE ONCOL 51 (2025) 100669

Contents lists available at ScienceDirect

Journal of Bone Oncology

journal homepage: www.elsevier.com/locate/jbo

Review

Diagnostic Innovations: Advances in imaging techniques for diagnosis and follow-up of multiple myeloma

M. Talarico [a,b], S. Barbato [a,b], A. Cattabriga [b,c], I. Sacchetti [a,b], E. Manzato [a,b], R. Restuccia [a,b], S. Masci [a,b], F. Bigi [a,b], M. Puppi [a,b], M. Iezza [a,b], I. Rizzello [a,b], K. Mancuso [a,b], L. Pantani [a], P. Tacchetti [a], C. Nanni [d], M. Cavo [b], E. Zamagni [a,b,*]

[a] IRCCS Azienda Ospedaliero-Universitaria di Bologna, Istituto di Ematologia "Seràgnoli", Bologna, Italy
[b] Dipartimento di Scienze Mediche e Chirurgiche, Università di Bologna, Bologna, Italy
[c] Department of Radiology, IRCCS Azienda Ospedaliero Universitaria di Bologna 40138 Bologna, Italy
[d] Nuclear Medicine, IRCCS Azienda Ospedaliero-Universitaria di Bologna, Bologna, Italy

HIGHLIGHTS

- WBLDCT is recommended as the first-choice imaging technique to assess bone disease in MM. ^{18}F-FDG-PET/CT is considered a possible alternative at staging and is recommended for imaging MRD assessment. In cases with no myeloma-defining events, the use of MRI is recommended.
- Dual energy CT has been proposed to overcome some limitations of WBLDCT, but its use is limited by lack of standardization.
- Novel PET radiotracers being studied in MM could overcome some limits of ^{18}F-FDG-PET/CT, but their use is limited by low availability and expertise, need of a local cyclotron for tracers with a short half-life, absence of standardization, and need for further prospective data.
- DCE -MRI allows to study tumor angiogenesis in a non-invasive way, but its use is limited by lack of clinical validation and standardized protocols.
- DWI represents a modern MRI protocol allowing to study cellular density of tissues, whose use in MM has been standardized by MY-RADS guidelines, both at staging and in response assessment.

ARTICLE INFO

Keywords:
Multiple Myeloma
Bone disease
Imaging
^{18}F-FDG-PET/CT
WB-DWI-MRI
DCE-MRI

ABSTRACT

Introduction: The International Myeloma Working Group (IMWG) defines myeloma related bone disease (MBD) as a diagnostic criterion for symptomatic multiple myeloma (MM) as the presence of osteolytic lesions $\geq$ 5 mm or more than one focal lesion (FL) $\geq$ 5 mm by magnetic resonance imaging (MRI). Whole-body low-dose CT (WBLDCT) is recommended as the first-choice imaging technique for the diagnosis of MBD with ^{18}F-fluorodeoxyglucose-positron emission tomography/CT (^{18}F-FDG-PET/CT) being considered a possible alternative at staging, whereas use of MRI studies is recommended in cases without myeloma-defining events (MDEs) in order to exclude the presence of FLs. Furthermore, use of ^{18}F-FDG-PET/CT is recommended in response assessment, to be integrated with hematologic response and bone marrow minimal residual disease (MRD).
Areas covered: In this paper, we review novel functional imaging techniques in MM, particularly focusing on their advantages, limits, applications and comparisons with ^{18}F-FDG-PET/CT or other standardized imaging techniques.
Conclusions: Combining both morphological and functional imaging, ^{18}F-FDG-PET/CT is currently considered a standard imaging technique in MM for staging (despite false positive or negative results) and response assessment. The introduction of novel functional imaging techniques, as whole-body diffusion-weighted magnetic resonance imaging (WB-DWI-MRI), or novel PET tracers might be useful in overcoming these limits. Future studies will give more information on the complementarity of these imaging techniques or whether one of them might become a new gold standard in MM.

* Corresponding author at: Dipartimento di Scienze Mediche e Chirurgiche, Università di Bologna, Via Massarenti, 9 - 40138 Bologna, Italy.
E-mail address: e.zamagni@unibo.it (E. Zamagni).

https://doi.org/10.1016/j.jbo.2025.100669
Received 21 December 2024; Received in revised form 18 February 2025; Accepted 19 February 2025
Available online 28 February 2025
2212-1374/© 2025 The Author(s). Published by Elsevier GmbH. This is an open access article under the CC BY-NC license (http://creativecommons.org/licenses/by-nc/4.0/).

1. Introduction

Myeloma-related bone disease (MBD) is a major cause of morbidity in patients affected by multiple myeloma (MM), affecting about 80% of patients with newly diagnosed MM (NDMM) and almost the totality of patients during the disease course [1,2]. These patients present with bone pain as the most common onset-symptom and are at high risk for skeletal-related events (SREs), including pathological fractures, spinal cord compression and need for surgical or radiotherapeutic interventions [3]. Furthermore, MM patients may present with paraskeletal disease (PSD) as a result of direct growth from bone lesions due to disruption of the cortical bone, or extramedullary disease (EMD), resulting from haematogenous spread involving soft tissues without direct contact to bone structures. The former has a reported incidence of 7–34.4% in NDMM patients and 6–34.2% in relapsed/refractory (RRMM) patients; the latter has a reported incidence of 1.7–4.5% in NDMM and 3.4–10% in RRMM [4].

In 2003, the International Myeloma Working Group (IMWG) defined MBD as a diagnostic criterion for NDMM requiring treatment initiation as the presence of osteolytic lesions or osteoporosis with compression fractures. Conventional skeletal radiography was the standard technique for diagnosis of MBD, with computed-tomography (CT) and magnetic resonance imaging (MRI) studies considered useful to improve its detection [5]. In 2014, the updated diagnostic criteria for MM clarified the definition of MBD as the presence of one or more osteolytic lesion ($\geq$ 5 mm in size) on skeletal radiography, CT or ^{18}F-fluorodeoxyglucose-positron emission tomography/CT (^{18}F-FDG-PET/CT) [6]. Since two studies in smoldering MM (SMM) have shown that the presence of more than one focal lesion (FL) detected by MRI was related to a progression rate to symptomatic MM of 70% at 2 years with a median time to progression (TTP) of 13–15 months [7,8] the updated IMWG diagnostic criteria for NDMM also include the presence of $>$ 1 FLs (each $\geq$ 5 mm in size) by MRI [6]. As whole-body low-dose CT (WBLDCT) has proven significantly superior sensitivity as compared to conventional skeletal survey in detecting osteolytic lesions [9] current IMWG guidelines (Fig. 1) recommend its use as the first-choice imaging technique for the diagnosis of MBD in MM patients. ^{18}F-FDG-PET/CT, if available, is considered a potential alternative to WBLDCT. If WBLDCT (or CT portion of PET/CT, as increased uptake only is not adequate for diagnosis of MM) is negative and no other myeloma defining event is present, the use of whole-body MRI (WB-MRI) is recommended. Alternatively, if WB-MRI is not available, patients should undergo MRI of spine and pelvis (axial skeleton MRI, AS-MRI) [10].

^{18}F-FDG-PET/CT, combining both morphological and functional imaging, has sensitivity and specificity of 80–100% for detection of bone lesions and is considered the most effective technique in identifying EMD (with the exception of central nervous system involvement, for which MRI studies are preferable). Furthermore, the presence of $>$ 3 FLs, of EMD, of high level of FDG uptake (maximum standardized unit value, SUV_{max}), high metabolic tumor volume (MTV) or total lesion glycolysis (TLG) have been related to inferior outcome [11–16]. Conversely, MRI studies are considered the techniques having the highest sensitivity in detecting early bone damage and diffuse involvement of bone marrow, in distinguishing pathological from osteoporotic fractures and in studying cord compression or other neurologic events [11,17–20].

Current IMWG guidelines recommend the integration of conventional hematologic response with the assessment of bone marrow minimal residual disease (MRD) by Next Generation Sequencing (NGS) or Next Generation Flow (NGF) [21]. However, evaluation of MRD is limited by potential spatial heterogeneity, patchy pattern of bone marrow and possible presence of EMD. Therefore, imaging techniques play a crucial role in response assessment. ^{18}F-FDG-PET/CT is considered the standard technique in this setting, as various studies have shown that normalization of tracer uptake is related to a significant improvement of patients outcomes [12–14,21–25]. For this reason, assessment of imaging MRD by ^{18}F-FDG-PET/CT is also recommended

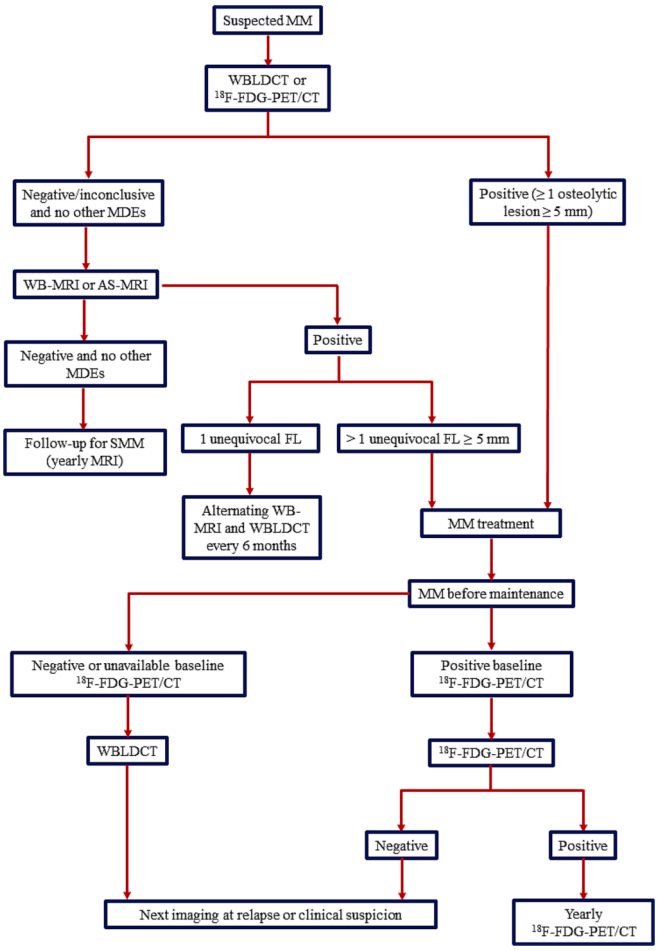

Fig. 1. Imaging algorithm for patients with suspected NDMM and for response evaluation during therapy; adapted from [10]. Abbreviations: NDMM = newly diagnosed multiple myeloma; WBLDCT = whole-body low dose computed tomography; ^{18}F-FDG-PET/CT = ^{18}F-fluorodeoxyglucose-positron emission tomography/computed tomography; WB-MRI = whole-body magnetic resonance imaging; AS-MRI = axial skeleton MRI; MDE = myeloma defining event; SMM = smoldering MM.

by IMWG guidelines [10,21]. PET negativity is defined as the disappearance of every area of increased tracer uptake previously found, decrease to less than mediastinal blood pool SUV or to less than surrounding normal tissue. However, the Italian group recently proposed a standardization of ^{18}F-FDG-PET/CT according to Deauville score (DS) (Italian Myeloma Criteria for PET Use, IMPeTUs criteria), finding that achievement of DS $<$ 4 (uptake lower than liver) for both FLs and bone marrow diffuse uptake is an independent predictor for improved progression-free survival (PFS) and overall survival (OS), hence proposing new definitions of metabolic responses [26,27]. The use of IMPeTUs criteria in response assessment and their integration with MRD evaluation have been recently validated in the "FORTE" trial, with double-negative patients achieving better outcome [28]. Conversely, even though early studies regarding use of conventional MRI studies in response assessment showed a prognostic significance of FLs resolution after therapy [18,29], a high rate of false-positive results (due to the persistence of visible necrotic lesions) has been reported and more recent trials failed to show a significant correlation with patients outcomes [12]. However, modern MRI protocols which will be described in the following chapters (i.e., dynamic contrast-enhanced, DCE, and diffusion-weighted imaging, DWI) are being successfully evaluated for response assessment.

In this paper, we review novel functional imaging techniques in MM,

particularly focusing on their advantages, limits, applications and comparisons with ^{18}F-FDG-PET/CT or other standardized imaging techniques.

2. Novel CT techniques

2.1. Dual-energy CT

Conventional CT studies, including WBLDCT (which currently represents the standard imaging technique in assessing MBD) are defined monoenergetic (single-energy computed tomography, SECT), as they are based on the use of a photon beam including a wide range of energies centered around a single peak. SECT techniques allow for a distinction of structures depending on different densities of tissues and attenuation coefficients, expressed in terms of Hounsfield Unit (HU). The Hounsfield scale ranges from values of −1000 HU for air to + 1000 HU for bone, with water representing the conventional 0. Blood volume and fat usually have values of approximately + 40 HU and −90/_70 HU, respectively [30]. However, diverse materials may have similar attenuation coefficients and be represented by identical pixel values. Dual-energy CT (DECT) is a new technology based on acquisition of images at different energies, based upon the use of two beams with diverse energies coming from two X-ray tubes (dual-energy spectral CT) or the use of two detectors for photons at different energies (dual-layer spectral CT), with specific attenuation depending on both photon energy level and tissue composition. Specific reconstruction algorithms allow for more precise material decomposition analysis and tissue characterization, based on the different attenuations at diverse beam energies [31–33].

In MM, one major limit of WBLDCT and other SECT studies is represented by a modest negative predictive value in detecting bone marrow involvement without lytic lesions. Conversely, calcium-suppressed (virtual non-calcium, VNCa) images from DECT, through three-material decomposition (calcium, water and fat) and modulation of calcium suppression index (CaSupp), allow the removal of the osseous component with qualitative and quantitative assessment of bone marrow composition and characterization of FLs; furthermore, a potential use in response assessment has been proposed [34–36].

Using MRI as reference standard, DECT has shown high sensitivity (91.3%) and specificity (90.9%) in assessing bone marrow infiltration; a cut-off value of −44.9 HU was related to a sensitivity of 93.3% and specificity of 92.4% in distinguishing normal from infiltrated bone marrow [37]. Another study allowed to distinguish normal bone marrow from diffuse infiltration (cut-off of −35.7 HU, with 100% sensitivity and 97% specificity) or from focal infiltration (cut-off of −31.9 HU, with 97% sensitivity and 99% specificity), again using MRI as reference standard [38]. Regarding detection of diffuse infiltration, some studies have also tried to assess the skeleton location having the best correlation to MRI, which was found to be L3 with CaSupp index 65 [39].

Use of VNCa images has also been proposed for differentiation of osteolytic FLs into active and inactive ones, as the former show higher attenuation: a cut-off value of −21 HU is related to a sensitivity of 92% and a specificity of 58%. A significant negative association to T1 weighted signal intensity and a positive association to apparent diffusion coefficient, ADC, by DWI-MRI studies has been observed [40]. A comparison of DECT and SECT highlighted the superiority of the former technique in distinguishing active FLs (by using ^{18}F-FDG-PET/CT as reference standard), with a significant correlation between attenuation and metabolic activity, particularly in images with high CaSupp index; a cut-off of −46.9 HU was related to a sensitivity of 91% and a specificity of 88% [41]. Another study observed a decreased attenuation from −4.5 HU to −53.5 HU (median values) in FLs responding to radiotherapy, likely reflecting fatty regression as a sign of response; conversely, locally progressive lesions showed higher attenuation (cut-off of −27 HU) [42].

Other studies have focused on identifying relations between characteristics of DECT imaging and markers of disease burden or prognostic features. For example, a positive correlation between calcium subtracted attenuation and bone marrow plasma cell infiltration percentage and a negative correlation with hemoglobin level has been observed. Furthermore, some studies showed a significant relation between specific CT textural features in VNCa images and serologic markers, or staging systems have been observed [43,44].

In addition to VNCa images, other studies have used a two-material decomposition with separation of hydroxyapatite (paired to fat or other materials) for the diagnosis of non-osteolytic MM, with better results obtained by grouping different spine segments [45,46].

However, the main limitation of DECT imaging in MM is represented by a great heterogeneity in the studies, regarding acquisition technologies, postprocessing software, qualitative classification criteria, measurement sites of skeleton and timepoints after treatment, concurring to difficult replication of results and standardization. Furthermore, this technique resulted ineffective in distinguishing bone marrow malignant infiltration from bone marrow reconversion [34].

2.2. Photon-counting CT

Another recently introduced technology is the photon-counting detector CT (PCD-CT), based on direct conversion of X-ray into electric impulses, with generation of multi-energy images having increased contrast, scanning speed and spatial resolution with lower image noise and radiation doses as compared to conventional CT techniques based on energy integrating detectors (EID-CT) [47].

A comparative study between PCD-CT and EID-CT in MM has shown a significant improvement in identifying osteolytic lesions, intramedullary lesions, fatty metamorphosis and pathologic fractures with the former technique [48]. Furthermore, a significant improvement in spatial resolution of bony microstructure and lytic bone lesions as compared to DECT has been observed [49].

3. Novel PET radiotracers

^{18}F-FDG is the most commonly used and standardized radiotracer for PET imaging in MM, with sensitivity and specificity ranging from 80% to 100% in detecting bone lesions. False positive FLs may result from infections and other causes of inflammation, post-surgical areas or biopsies, fractures, bone remodeling, bone metallic implants, accumulation of the radiotracer in physiological districts, whereas anemia or recent chemotherapy, radiotherapy and growth factors may cause a false diffuse bone marrow pattern. Conversely, false negative results may be due to hyperglycemia, recent high-dose corticosteroid administration, small skull lesions close to the brain, or lacking expression of glucose transporters or enzymes involved in glycolysis (particularly hexokinase-2), which has been reported in about 10% of patients, being not stable over time and potentially changing during the disease course [50,51]. To overcome these limitations, other radiotracers have been investigated (Table 1), with some having possible theranostic implications.

3.1. Chemokine receptor tracer

C-X-C motif chemokine receptor 4 (CXCR4) is a G protein-coupled receptor resulting overexpressed in about half of MM patients [52,53]. It plays a crucial role in cell migration and homing, angiogenesis and proliferation, via interaction with C-X-C motif chemokine ligand 12 (CXCL12), expressed on bone marrow stromal cells. Furthermore, its overexpression in MM has been related to increased osteoclastogenesis [54]. Pentixafor is a peptidomimetic ligand with high affinity for CXCR4 which has been conjugated with ^{68}Ga (^{68}Ga-PEN) and evaluated in MM, showing promising results in detection of active disease and in prognostic stratification. In a retrospective analysis of RRMM patients, ^{68}Ga-PEN-PET/CT was positive in 66% of patients, independently from laboratory parameters or cytogenetics. In 42% of patients, it detected the same number of lesions as ^{18}F-FDG-PET/CT, whereas it resulted superior

Table 1
Novel PET radiotracers in MM.

Class of radiotracer	Target and rationale	Radiotracer	Summary of findings and comments
Chemokine receptor	CXCR4 (high expression on MM plasma cells related to migration, homing, proliferation, angiogenesis and osteoclastogenesis)	^{68}Ga-Pentixafor	Positivity rate of 66–93%; significant superiority versus ^{18}F-FDG for BM DD; false negative scans up to 16%; potential prognostic role [55,56,58]
Amino acids tracers	Amino acid metabolism (high uptake by plasma cells due to immunoglobulin production)	^{11}C-methionine	Higher positivity rate (up to 91%), sensitivity and number of FLs than ^{18}F-FDG; potential prognostic role; short half-life [65,66]
		^{18}F-fluoro-ethyl-tyrosine	Lower uptake than ^{18}F-FDG and ^{11}C-MET [69]
		^{18}F-fluciclovine	Higher positivity rate (92%) than ^{18}F-FDG [70]
Lipid tracers	Integration in cell membrane of replicating cells	^{11}C-choline	Higher number of FLs than ^{18}F-FDG but lower than ^{11}C-methionine; short half-life [71,72]
		^{18}F-choline	Higher number of FLs than ^{18}F-FDG [73,74]
	Integration in cell membrane of replicating cells and fatty acid metabolism	^{11}C-acetate	Higher positivity rate (85%) than ^{18}F-FDG, particularly for BM DD (up to 100%); potential prognostic role [75–77]
Nucleoside tracers	Thymidine kinase activity (uptake in proliferating cells)	^{11}C-thiothymidine	Encouraging preliminary results: higher positivity rate, sensitivity and negative predictive value than ^{18}F-FDG [78]
		^{18}F-fluorothymidine	Lower positivity rate and smaller number of FLs than ^{18}F-FDG [79]
Markers of hypoxia and vascular proliferation	Aberrant angiogenesis in MM	^{68}Ga-PSMA	Discordant preliminary results [80,81]
		^{18}F-fluoroarabinofuranosyl-2-nitroimidazole	Lower positivity rate than ^{18}F-FDG [82]
Bone matrix tracers	Osteoblastic activity	^{18}F-sodium-fluoride	Lower specificity than ^{18}F-FDG [83,84]
	Fibroblast inhibition	^{68}Ga-fibroblast activation protein inhibitor	No significant superiority versus ^{18}F-FDG [86]
Antibody tracers	CD38 (plasma cells' marker)	^{89}Zr-deferoxamine-Daratumumab	Encouraging preliminary data [87]

Abbreviations: PET = positron emission tomography; MM = multiple myeloma; CXCR4 = C-X-C motif chemokine receptor 4; PSMA = prostate-specific membrane antigen; FDG = ^{18}F-fluorodeoxyglucose; BM = bone marrow; DD = diffuse disease; FL = focal lesion.

in 21% and inferior in 37%. However, 16% of patients had CXCR4-negative disease even though having metabolic activity by ^{18}F-FDG-PET/CT[55]. Similar results have been observed in prospective comparisons to ^{18}F-FDG-PET/CT in NDMM patients. One experience showed a positivity rate of 93% versus 53% and a significant superiority in detecting bone marrow involvement (88% versus 29%) with marrow uptake values by ^{68}Ga-PEN-PET/CT resulting significantly correlated with presence of end organ damage, staging and laboratory markers of tumor burden, including concentration of serum and urine light chains and serum β2-microglobulin [56]. Another study showed a higher, similar and lower disease extent by ^{68}Ga-PEN in 68%, 26% and 6% of patients, respectively, with good concordance in detection of EMD. Moreover, tumor to background ratio was significantly correlated with bone marrow plasma cells percentage [57]. A significant relation between ^{68}Ga-PEN-PET/CT positivity and reduced overall survival has also been documented [58]. Due to these observations, endoradiotherapy (ERT) using Pentixather conjugated with ^{177}Lu and ^{90}Y (followed by hematopoietic stem cell transplantation because of bone marrow ablation) has been investigated in heavily pretreated patients, showing promising efficacy and good tolerability [59–61].

3.2. Amino acid tracers

Due to rapid internalization of amino acids by MM cells involved in immunoglobulin production, various amino acid tracers have been developed.

Methionine conjugated with ^{11}C (^{11}C-MET) is characterized by significant absorption by plasma cells (both in intramedullary and extramedullary lesions) as compared to bone marrow [62,63]. Comparisons between ^{11}C-MET and ^{18}F-FDG-PET/CT have shown higher sensitivity and accuracy of the amino acid tracer [64]. In a study comparing the two radiotracers in NDMM and RRMM, ^{11}C-MET had a higher percent positive (91% versus 77%) and detected more FLs in 65% of patients, whereas the two tracers identified the same number of FLs in the remaining 35% of patients. Furthermore, a stronger correlation with bone marrow involvement as compared to ^{18}F-FDG was observed [65]. Similar results were produced in a double-center prospective trial enrolling both NDMM and RRMM patients: 12% of patients had a PET/CT resulting negative by ^{18}F-FDG but positive by ^{11}C-MET whereas no patients had metabolically active disease only by ^{18}F-FDG-PET/CT; the amino acid tracer detected more FLs in 63% of patients. In this study, various semiquantitative parameters by ^{11}C-MET-PET/CT were significantly correlated to patients outcomes [66]. Moreover, a small study recently showed a potential role of ^{11}C-MET-PET/CT in detecting persistent active disease in patients having negative ^{18}F-FDG-PET/CT after treatment [67]. However, use of ^{11}C-MET is limited by its short half-life (20 min), necessitating the presence of on-site cyclotron [68].

Two further amino acid tracers which have recently been evaluated in MM are fluoro-ethyl-tyrosine and fluciclovine, both conjugated with ^{18}F (^{18}F-FET and ^{18}F-FACBC, respectively). Both tracers have a long half-life (110 min), not requiring a local cyclotron. The former, recently investigated for diagnosis of brain tumors, has shown lower uptake than ^{18}F-FDG and ^{11}C-MET in plasma cells lines [69]. The latter, commonly used for imaging of prostate cancer, has been compared to ^{18}F-FDG in NDMM patients in a small prospective study, showing higher positivity rate (92% versus 69%), with higher uptake values and number of FLs. Furthermore, SUV_{max} by ^{18}F-FACBC was significantly related to percentage of bone marrow plasma cells [70].

3.3. Lipid tracers

Use of lipid tracers, due to integration in cell membrane of replicating plasma cells, has also been evaluated. Choline (CH), conjugated with ^{11}C (^{11}C-CH) is a radiotracer used for prostate cancer imaging, limited by a short half-life (20 min). A comparison to ^{18}F-FDG in MM demonstrated detection of a higher number of bone lesions, with non-significant difference [71]. A subsequent comparison to ^{11}C-MET-PET/CT, however, showed higher sensitivity of the amino acid tracer with detection of more intramedullary lesions in 42% of patients [72]. Use of ^{18}F-CH, characterized by longer half-life (110 min), has been investigated in NDMM and at suspect of relapse, with detection of a higher number of FLs and higher SUV_{max} values as compared to ^{18}F-FDG in both settings [73,74].

Acetate is converted by human cells to acetyl-CoA, which is

incorporated in cell membrane or participates to the tricarboxylic acid cycle. For these reasons, ^{11}C-AC has been recently investigated both in neoplastic diseases and in evaluation of myocardial perfusion and oxygen consumption. A comparison to ^{18}F-FDG in plasma cell dyscrasias revealed a higher percentage positive for diffuse and focal active disease (85% versus 58%) [75]. Another study confirmed a higher detection of diffuse disease as compared to ^{18}F-FDG (100% versus 40%) and showed a reduction of mean SUV_{max} resulting proportional to the depth of hematologic response after treatment [76]. Furthermore, diffuse AC uptake has resulted significantly related to greater plasma cell infiltrate in bone marrow, higher staging and several markers of disease burden, including hemoglobin, concentration of M protein; moreover, the presence of high SUV_{max}, high number of FLs and diffuse uptake could predict shorter PFS [75,77].

3.4. Other novel radiotracers

Due to increased uptake in proliferating cells, nucleoside tracers (^{11}C-thiothymidine and ^{18}F- fluorothymidine, ^{18}F-FLT) have also been compared to ^{18}F-FDG in small studies. The former showed higher positivity rate, sensitivity (93% versus 60%) and negative predictive value (94% versus 73%) than ^{18}F-FDG [78]. Conversely, the latter was related to lower positive cases and detection of a smaller number of FLs, with high background activity in the bone marrow complicating the evaluation of lesions [79].

Radiotracers related to hypoxia and angiogenesis are also currently investigated. Prostate-specific membrane antigen (PSMA), conjugated to ^{68}Ga (^{68}Ga-PSMA) is a marker of vascular proliferation and represents the standard tracer for prostate imaging. Its comparison to ^{18}F-FDG in MM has produced discordant results: one study suggested a possible complementarity, demonstrating detection of higher number of FLs by ^{18}F-FDG (84% versus 71%) with 16% of FLs detected only by ^{68}Ga-PSMA and 29% only by ^{18}F-FDG and good reliability for number of FLs, number of soft tissue lesions and highest SUV_{max} [80]. Conversely, our experience highlighted a significant superiority of ^{18}F-FDG versus ^{68}Ga-PSMA regarding percent positive (68% versus 51%, with 19.5% of patients having positive ^{18}F-FDG but negative ^{68}Ga-PSMA and only 2% of patients having positive ^{68}Ga-PSMA but negative ^{18}F-FDG), detection of FLs and bone marrow diffuse uptake in NDMM patients [81]. Use of ^{18}F-FAZA (fluoroarabinofuranosyl-2-nitroimidazole, a marker of tumor hypoxia) produced negative results [82].

Sodium-fluoride conjugated with ^{18}F (^{18}F-NaF) is a tracer of osteoblastic activity, as it is chemo-adsorbed to hydroxyapatite. Various studies comparing ^{18}F-NaF-PET/CT to ^{18}F-FDG-PET/CT have demonstrated higher specificity of the latter for detecting osteolytic FLs in MM, likely due to osteoclastic role in their pathogenesis [83 84]. However, a potential complementarity because of its role in assessing degenerative bone fractures has been proposed [85].

Further radiotracers of recent investigation in MM are fibroblast activation protein inhibitor conjugated with ^{68}Ga (^{68}Ga-FAPI), which did not result superior to ^{18}F-FDG [86] and Daratumumab conjugated with ^{89}Zr using deferoxamine (^{89}Zr-DFO-Dara), recently related to encouraging results [87].

Even though potentially attractive, use of novel PET radiotracers harbors some limitations, which are both technical (low availability and expertise, need of a local cyclotron for tracers with a short half-life) and conceptual (absence of standardization, need of further prospective data about eventual increased baseline sensitivity and use for response assessment).

4. Dynamic contrast-enhanced magnetic resonance

Conventional MRI represents the gold standard technique in detecting early bone marrow infiltration, with high sensitivity in assessing the presence of FLs and diffuse disease [88]. Further improvement in sensitivity has been achieved through the introduction of gadolinium as a contrast agent, particularly in DCE images, which allow to study tumor angiogenesis in a non-invasive way. This functional protocol is based on high temporal resolution repeated scanning (using T1-weighted sequences of dorsolumbar spine) before, during and after gadolinium administration. Changes in local perfusion over time, evaluated through time-intensity curves (TICs), reflect changes in bone marrow microcirculation, due to angiogenesis and increased vascular permeability. Two main perfusion parameters are studied: amplitude A (reflecting blood volume) and exchange rate constant Kep (reflecting vessel wall permeability). Wash-in and wash-out features allow distinction of 5 different patterns of TICs (Fig. 2). Symptomatic MM is usually characterized by type 4 TIC, due to a steep wash-in and first pass (reflecting immediate unidirectional flow from intravascular to interstitial space because of angiogenesis with marked microvascular density and vessel permeability) and a rapid wash-out (reflecting a retrograde flow towards intravascular space, because of small interstitial space due to high cellular density). MM patients rarely show type 5 TIC, with steep but continuous wash-in (reflecting the persistence of large interstitial space) [89–91].

DCE-MRI studies allow to detect a gradual progressive increase of microcirculation from MGUS to SMM to MM, with a progressive increase of peak enhancement intensity (PEI) and decrease of time to PEI (TPEI) [92,93]. Furthermore, higher amplitude A in SMM patients was revealed as a risk factor for progression to symptomatic MM (value above 0.89 arbitrary units is related to a progression rate of 80% at 2 years), whereas no prognostic role was found in patients with MGUS [94]. Findings of greater vascularization were also related to a significantly inferior outcome in patients with symptomatic MM: higher amplitude A was related to a greater incidence of non-response to therapy [95] and worse EFS [96]. Both higher amplitude A and Kep were related to a significantly worse OS [97]. Furthermore, patients with a diffuse disease by PET or DWI-MRI are characterized by significantly higher PEI and lower TPEI [93].

DCE-MRI studies have also been evaluated in response assessment. In patients responding to therapy, a decrease of 73% in wash-in slope and 71% in absolute enhancement (reaching a type 1 or type 2 TIC) can be detected, reflecting the destruction of tumor vascularization due to effective treatment. However, patients achieving a good hematologic response may show a type 3 TIC (characterized by steep wash-in and subsequent plateau), likely due to increased vascularization after hematopoiesis regeneration, because of anti-clone treatment or administration of stimulating-agents [92,98]. Furthermore, the evaluation of maximal percentages of bone marrow enhancement after treatment could be used in response assessment: a post-treatment value above 96.8% resulted predictive of non-response with a sensitivity of 100%

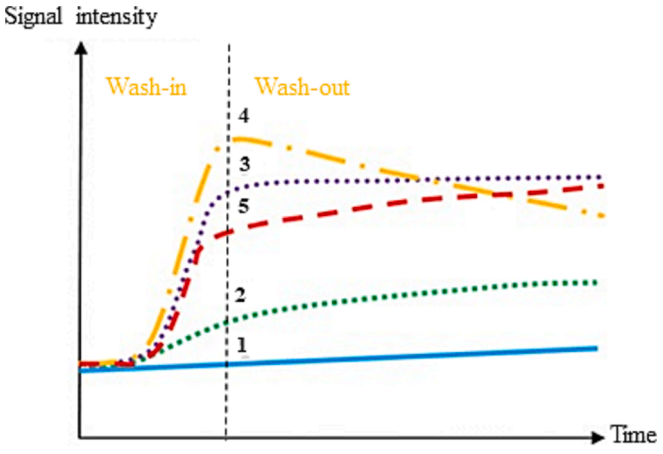

Fig. 2. Types of TICs by DCE-MRI; adapted from [90]. Abbreviations: TICs = time-intensity curves; DCE-MRI = dynamic contrast-enhanced magnetic resonance imaging.

and specificity of 77% after autologous stem cell transplant (ASCT). Conversely, the maximal percentage of focal lesion enhancement after therapy was not revealed prognostic [99]. Moreover, a study found that patients with deeper hematologic responses had significantly lower values of amplitude A and Kep as compared to non-responding patients [95].

Even though encouraging, use of DCE-MRI is actually limited by lack of clinical validation and standardized protocols (particularly considering the variability due to amount of contrast agent injected, scan duration and time resolution). Another limit of DCE-MRI is the need of adjusting results for age, sex, body mass index and other variables which may impact on bone marrow vascularization [100]. Furthermore, it should be highlighted use of gadolinium in patients with baseline impairment of kidney function has been related to an increased risk of nephrogenic systemic sclerosis [101].

5. Whole-body diffusion-weighted magnetic resonance

DWI represents a modern MRI protocol measuring the movement of water molecules within a tissue, which is inversely correlated to its cellular density. Its use has been related to high sensitivity in assessment of bone marrow infiltration and has been proposed for response assessment. MY-RADS (Myeloma Response Assessment and Diagnosis System) guidelines have been recently published with the aim of standardizing acquisition, interpretation and reporting of this technique in MM [102]. This protocol is based on a WB field of view (skull vertex to knees) using both conventional morphological sequences (T1-weighted, T2-weighted and short T1 inversion recovery – STIR – with section thickness of 4–5 mm) and specific ones (DWI and T1-weighted sequences with Dixon technique for fat-suppression), without need for contrast agents and a duration of 40–60 min. DWI technique relies on qualitative parameters (particularly the comparison with adjacent muscle, using high b-value images, generally 900 s/mm^2) and semi-quantitative approaches (ADC, which has been significantly related to the grade of histological infiltration by malignant cells and microvascular density) [102,103].

5.1. DWI-MRI at staging

ADC values of normal bone marrow are generally below 600–700 μm^2/s (due the presence of fat yellow marrow, with decreasing values in older people), whereas values of viable tumor are generally between 700 and 1400 μm^2/s (Fig. 3). Four disease patterns have been described: focal (lesions greater than 5 mm with decreased signal in T1-weighted sequences, increased signal in T2-weighted and STIR sequences, hyperintense to background muscle in high b-value images, compatible ADC values), micronodular (widespread nodular areas below 5 mm with preserved normal marrow between them), diffuse (diffuse decreased signal intensity in T1-weighted sequences and increased signal intensity in T2-weighted, STIR and high b-value DWI sequences, with ADC values above 600–700 μm^2/s), and focal on diffuse. Furthermore, WB-DWI-MRI represents a good tool for detection of PSD and EMD [102]. Beside evaluation of ADC maps regarding FLs and bone marrow infiltration, the use of volumetric quantitative parameters has been proposed: total diffusion volume (TDV), a measure of tumor burden, is evaluated by measuring the voxels with abnormal ADC values [104].

A recent *meta*-analysis regarding DWI-MRI at baseline diagnosis and staging reported a pooled sensitivity and specificity of 86% and 63% respectively, with a significant superiority as compared to conventional MRI studies [105]. Early comparisons to ^{18}F-FDG-PET/CT have shown higher sensitivity of WB-DWI-MRI in detecting both FLs and diffuse disease, with significant superiority in all anatomic regions, with the exception of the skull [106–109]. Furthermore, a similar sensitivity in detecting EMD has been reported [108]. The biggest retrospective study (46 NDMM patients) showed a significantly higher sensitivity of DWI-MRI in detecting FLs (91% versus 70%), but underlined that performing this technique in addition to ^{18}F-FDG-PET/CT does not significantly change treatment decisions [110]. "iTIMM", the biggest prospective trial in this setting (60 NDMM patients), confirmed the superiority of WB-DWI-MRI, showing the presence of FLs and diffuse disease in 83% versus 60% and 82% versus 17% of patients, respectively. In this study, WB-DWI-MRI was more sensitive as compared to ^{18}F-FDG-PET/CT in all anatomic regions, except ribs, scapulae and clavicles [111]. Early results on 54 NDMM patients from our prospective experience have confirmed the superiority of WB-DWI-MRI versus ^{18}F-FDG-PET/CT in detecting FLs (76% versus 54%) and PSD (30% versus 20%), whereas a slight

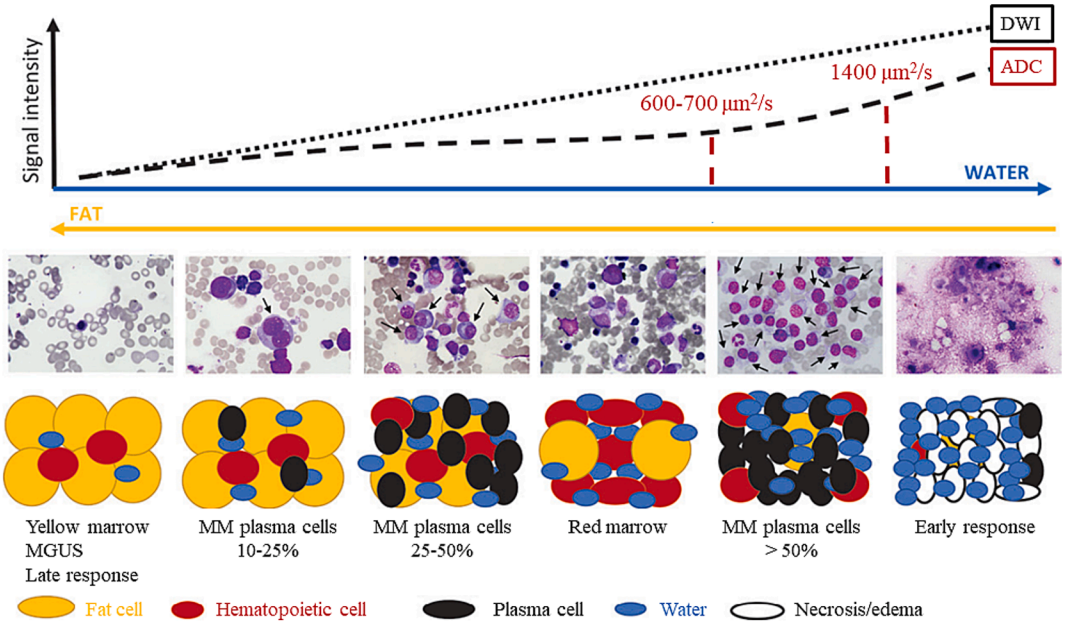

Fig. 3. Relation between ADC values, signal intensity in DWI sequences and bone marrow cellular density during disease course and response to therapy; adapted from [90] and [137]. Abbreviations: ADC = apparent diffusion coefficient; DWI = diffusion-weighted imaging; MGUS = monoclonal gammopathy of undetermined significance; MM = multiple myeloma.

concordance in detecting diffuse disease was observed [112].

5.2. Prognostic value of DWI-MRI

Prognostic value of baseline DWI-MRI has also been investigated. A study showed that presence of at least 3 large FLs with product of perpendicular diameters > 5 cm^2 is significantly associated with poor PFS and OS, independently from staging (Revised International Staging System, R-ISS), genetic risk and presence of EMD. The number of FLs lost its prognostic impact after adjusting for size of FLs, highlighting the role of high tumor burden [113]. Furthermore, the presence of a high TDV has been significantly related to high bone marrow plasma cell volume and to worse outcome [114]. Moreover, the presence of a diffuse disease has been related to the presence of several markers of disease burden and prognosis, including high R-ISS, higher plasma cell infiltration, higher M−protein concentration, lower hemoglobin level [111,112]. In one study, all patients with a diffuse disease had high-risk genetics [111]. Conversely, analysis of eventual prognostic role of ADC values have produced discordant results [115–117].

5.3. DWI-MRI in response assessment

WB-DWI-MRI has also been recently proposed for response assessment. Indeed, in patients responding to therapies, conventional MRI can show decrease in number and size of FLs, conversion of bone marrow pattern from diffuse to focal, combined or normal, or from focal or combined to normal, increase of signal intensity in T1-weighted sequences due to fat conversion around or within the lesions (“fat dot” and “halo sign”), decrease of signal intensity in T2-weighted or STIR sequences and reduced contrast uptake [34]. Moreover, Dixon sequences may highlight fat reconversion; some studies have shown a significantly higher increase of marrow fat fraction in patients responding to therapy as compared to non-responders [118,119]. Furthermore, a significant change of ADC values in responding lesions is observed through DWI sequences, as highlighted by comparison of pre- and post-treatment ADC histograms. Early evaluations show increased ADC values (due to tumor necrosis, microbleeding and edema, leading to a decrease of cellular density), whereas later evaluations show decreased ADC values because of fat reconversion (Fig. 3). Increase of ADC value after treatment has been significantly related to the presence of a biochemical response in various experiences [120–122] and has been related to sensitivity and specificity of 78% and 73% respectively in distinguishing responding patients by a recent *meta*-analysis [105]. Different cut-off values (with an increase of 30–40% from baseline) have been proposed, with a great limitation represented by the use of heterogeneous b-values. MY-RADS guidelines have recently defined 5 response assessment categories (RACs). In addition to morphologic changes, response is characterized by increase od ADC values from ≤ 1400 μm^2/s to > 1400 μm^2/s or a relative increase $\geq 40\%$ from baseline values. It should be highlighted that RACs aim at distinguishing different probability of response or progression after treatment, ranging from RAC1 (highly likely to be responding) to RAC5 (highly likely to be progressing) [102]. This approach differs from IMPeTUs criteria, recently proposed for response assessment by ^{18}F-FDG-PET/CT, which are based on a dichotomized classification between responders and non-responders [27] (Table 2).

Furthermore, a study showed a progressive decrease of TDV, resulting directly proportional to the depth of haematologic response (decrease of median TDV from 231.5 mL to 31.7 mL after treatment in the whole cohort, 90.56 mL in patients achieving $<$ CR and 27.56 mL in patients achieving $\geq$ CR) [123,124]. Moreover, a recent study proposed the use of a “combined skeletal score”, based on the integration of morphological and functional MRI data (from both DCE and DWI studies) to improve response assessment in MM patients, particularly in confirming the achievement of CR and in predicting relapse in apparently good-responding patients [98].

A single center prospective study assessed the role of an early

Table 2
PET and WB-DWI-MRI response criteria; and .

Metabolic response	Description	RACs	Description
Complete metabolic response (CMR)	Uptake $\leq$ liver activity in BM sites and FLs previously involved, including PSD and EMD (DS 1–3)	RAC1	Highly likely to be responding: - Return of normal fat containing marrow in areas previously infiltrated by FLs or DD; - Unequivocal decrease in number or size of FLs; - Conversion of a packed BM infiltrate into discrete nodules, with unequivocal decrease in tumor load in the respective BM space; - Decreasing soft tissue associated with bone disease; - Emergence of intra- or peritumoral fat within/around FLs (fat dot or halo sign); - Previously evident lesion shows increase in ADC from ≤ 1400 μm^2/sec to > 1400 μm^2/sec; - $\geq 40\%$ increase in ADC from baseline with corresponding decrease in normalized high b-value signal intensity; morphologic findings consistent with stable or responding disease; - For soft-tissue disease, RECIST version 1.1 criteria for CR (disappearance of all TLs) / PR ($\geq 30\%$ decrease in the sum of LD of TLs, taking as reference the baseline sum LD)
Partial metabolic response (PMR)	Decrease in number and/or activity of BM/FLs present at baseline, but persistence of lesion(s) with uptake $>$ liver activity (DS 4–5)	RAC2	Likely to be responding: - Evidence of improvement but not enough to fulfill criteria for RAC1, for example slight decrease in number/size of FLs, previously evident lesions showing increases in ADC from ≤ 1000 μm^2/sec to < 1400 μm^2/sec, 25–40% increase in ADC from baseline with corresponding decrease in b-value signal intensity and morphologic findings consistent with stable or responding disease; - For soft-tissue disease, RECIST version 1.1 criteria not meeting requirements for PR
Stable metabolic disease (SMD)	No significant change in BM/FLs compared with baseline	RAC3	No change: - No observable change
Progressive metabolic disease (PMD)	New FLs consistent with MM compared with baseline	RAC4	Likely to be progressing: - Evidence of worsening disease, but not enough to fulfill criteria for RAC5; - Equivocal appearance of new lesion(s); - No change in size but increasing signal intensity

(*continued on next page*)

Table 2 (*continued*)

Metabolic response	Description	RACs	Description
			on high b-value images (with ADC values < 1400 μm^2/sec) consistent with possible disease progression; - Relapsed disease: reemergence of lesion(s) that previously disappeared or enlargement of lesion(s) that had partially regressed/stabilized with prior treatments; - Soft tissue in spinal canal causing narrowing not associated with neurologic findings ant not requiring radiation therapy; - For soft-tissue disease, RECIST version 1.1 criteria not meeting requirements for PD
		RAC5	Highly likely to be progressing: - New critical fracture(s)/ cord compression requiring radiation therapy/surgical intervention; only if confirmed as malignant with MRI signal characteristics; - Unequivocal new focal [5–10] diffuse area(s) of infiltration in regions of previously normal marrow; - Unequivocal increase in number/size of FLs; - Evolution of FLs to diffuse neoplastic pattern; - Appearance/increasing soft tissue associated with bone disease; - New lesions/regions of high signal intensity on high b-value images with ADC value between 600–1000 μm^2/sec; - For soft-tissue disease, RECIST version 1.1 criteria meeting requirements for PD (≥ 20% increase in the sum of LD of TLs, taking as reference the smallest sum LD recorded since the treatment started, or the appearance of ≥ 1 new lesion(s)

Abbreviations: RACs = response assessment categories; BM = bone marrow; FL = focal lesion; PSD = paraskeletal disease; EMD = extramedullary disease; DS = Deauville score; MM = multiple myeloma; DD = diffuse disease; ADC = apparent diffusion coefficient; CR = complete response; PR = partial response; LD = longest diameter; TL = target lesion; PD = progressive disease.
adapted from [27][102]

evaluation (after one cycle of induction therapy), finding no significant changes in ADC values between patients achieving at least a very good partial response (VGPR) or less than VGPR, whereas significant changes in fat fraction metrics were identified [125]. Early results from our prospective experience in NDMM patients have shown a good concordance (87.5%) between ^{18}F-FDG-PET/CT and WB-DWI-MRI in response assessment (before maintenance therapy for patients undergoing ASCT or after 1 year of therapy for transplant-ineligible patients) [112]. A recent prospective comparison between these two imaging techniques in response assessment after induction therapy and after ASCT showed a significant impact on patient outcome (PFS and OS) of a positive PET scan at both time-points, whereas absence of response using MY-RADS criteria did not affect patient outcome [115]. Conversely, a study not using standardized criteria has shown a significantly inferior outcome in patients reaching a hematologic complete response (CR) but with persisting FLs by ^{18}F-FDG-PET/CT or DWI-MRI. In this study, DWI-MRI identified more residual FLs as compared to PET, but some FLs were only PET positive, underlying a potential complementarity of the two techniques [126]. Another study in NDMM patients showed that achievement of RAC1 after ASCT and sustained RAC1 after 1 year are related to a significant improvement of both PFS and OS [127,128]. A *meta*-analysis has compared ^{18}F-FDG-PET/CT and WB-MRI (with DWI included in 5/12 studies) in response assessment, showing a significantly superior specificity of ^{18}F-FDG-PET/CT (81% versus 56%) and a non-significant superior sensitivity of WB-MRI (90% versus 66%). Use of DWI has been related to a non-significant improvement of sensitivity as compared to conventional WB-MRI (93% versus 74%), with comparable specificity [129]. Some recent studies have also proposed an integration of response assessment by DWI-MRI to bone marrow MRD evaluation, with double-negative patients achieving a better outcome as compared to patients with positive imaging or MRD and to double-positive patients [126,127,130]. Due to high diagnostic sensitivity and good performance at response assessment, British guidelines recommend the use of WB-MRI as gold standard imaging technique and propose it as an alternative to ^{18}F-FDG-PET/CT in response assessment [131,132]. However, it should be highlighted that use of DWI-MRI in response assessment is limited by the complexity of RACs. Therefore, new software and algorithms (even using artificial intelligence) with the aim of simplifying its use are on development. Table 3 provides a summary comparison between the main features of ^{18}F-FDG-PET/CT and WB-DWI-MRI.

Table 3
Main features of ^{18}F-FDG-PET/CT and WB-DWI-MRI in MM (references in text).

	^{18}F-FDG-PET/CT	WB-DWI-MRI
Scanning time	15–20 min (60 min after tracer infusion)	40–60 min
Radiation exposure	10–25 mSv	None
Diffuse bone marrow involvement	Lower sensitivity	Higher sensitivity
Detection of FLs	Lower sensitivity	Higher sensitivity
Detection of PSD	Lower sensitivity	Higher sensitibity
Detection of EMD	Gold standard technique	Less explored role
Prognostic features	> 3 FLs, high SUV_{max}, other quantitative parameters (MTV, TLG)	Diffuse disease, > 3 large (> 5 cm^2) FLs, high TDV, discordant data about ADC
Role in response assessment	Gold standard technique (IMWG); recent IMPeTUs criteria for definition of metabolic responses (prognostic role of DS < 4)	Preferred technique for British guidelines (MY-RADS criteria: prognostic role of RAC1)

Abbreviations: ^{18}F-FDG-PET/CT = ^{18}F-fluorodeoxyglucose-positron emission tomography/computed tomography; WB-DWI-MRI = whole-body diffusion-weighted magnetic resonance imaging; FLs = focal lesions; PSD = paraskeletal disease; EMD = extramedullary disease; SUV = standardized uptake value; MTV = metabolic tumor volume; TLG = total lesion glycolysis; TDV = total diffusion volume; ADC = apparent diffusion coefficient; IMWG = International Myeloma Working Group; IMPeTUs = Italian Myeloma Criteria for PET Use; DS = Deauville score; MY-RADS = Myeloma Response Assessment and Diagnosis System; RAC = response assessment category.

6. WB-PET/MRI

WB-PET/MRI (using ^{18}F-FDG as radiotracer) is a hybrid imaging technique actually being evaluated in MM. The main advantages of this technique include the possibility of concomitant evaluation of morphology, vascularization, bone marrow cellular density and metabolic activity. However, it is expensive and requires double expertise. Few data are available regarding its use in MM patients [34].

A prospective comparative study to ^{18}F-FDG-PET/CT showed equivalent concordance between the two techniques in detecting FLs, with a strong correlation regarding tracer uptake quantification (even though SUV values were significantly lower for PET/MRI) [133]. Another study at staging of newly-diagnosed plasma cell dyscrasias demonstrated sensitivity, specificity and accuracy of 93%, 97% and 95% respectively in detection of FLs and 98%, 66% and 79% respectively in detecting diffuse disease; these results were comparable to WB-DWI-MRI and superior to PET/CT, without achievement of a significantly increased diagnostic performance by adding DCE imaging [134]. A prospective French trial enrolling NDMM patients compared the diagnostic performance of this hybrid technique to PET and MRI separately, showing an equally effective accuracy regarding detection of FLs and diffuse disease in symptomatic patients, but a superiority of MRI in SMM (with detection of FLs in 22% of patients) [135]. Furthermore, a recent study has evaluated the prognostic role of PET/MRI in response assessment, showing that concomitant negativity of PET (DS $\leq$ 3) and WB-DWI-MRI (RAC1) after ASCT is related to improved PFS as compared to persistent positivity in one technique, particularly in case of MRI-positivity [136].

7. Conclusions

^{18}F-FDG-PET/CT is currently considered a standard imaging technique in MM, as it combines morphologic data (through its WBCT portion, representing the recommended technique for MBD assessment) and functional imaging (having a well-recognized role in prognostic stratification and response assessment, with standardized response criteria). However, use ^{18}F-FDG-PET/CT harbors some limitations, with various causes of false positive or negative results. The introduction of novel WB functional imaging techniques or novel PET tracers might be useful in overcoming these limits. Particularly, WB-DWI-MRI, even though limited by slight availability, appears very promising. Indeed, various studies have shown higher sensitivity of this technique as compared to ^{18}F-FDG-PET/CT in detecting FLs and bone marrow diffuse disease and a potential role in response assessment, thus overcoming the major limitation of conventional MRI. Future studies will have to further investigate the complementarity of these imaging techniques and to address whether they might be alternatively used (similarly to NGS and NGF in MRD assessment) or whether one of them might become a new gold standard.

CRediT authorship contribution statement

M. Talarico: Writing – original draft, Investigation, Formal analysis, Data curation, Conceptualization. **S. Barbato:** Writing – review & editing, Writing – original draft, Investigation. **A. Cattabriga:** Writing – review & editing, Investigation. **I. Sacchetti:** Writing – review & editing, Investigation. **E. Manzato:** Writing – review & editing, Investigation. **R. Restuccia:** Writing – review & editing, Investigation. **S. Masci:** Writing – review & editing, Investigation. **F. Bigi:** Writing – review & editing, Investigation. **M. Puppi:** Writing – review & editing, Investigation. **M. Iezza:** Writing – review & editing, Investigation. **I. Rizzello:** Writing – review & editing, Investigation. **K. Mancuso:** Writing – review & editing, Investigation. **L. Pantani:** Writing – review & editing, Investigation. **P. Tacchetti:** Writing – review & editing, Investigation. **C. Nanni:** Writing – review & editing, Investigation. **M. Cavo:** Writing – review & editing, Supervision, Investigation, Conceptualization. **E. Zamagni:** Writing – review & editing, Supervision, Resources, Project administration, Funding acquisition, Conceptualization.

Declaration of competing interest

The authors declare that they have no known competing financial interests or personal relationships that could have appeared to influence the work reported in this paper.

IR has received honoraria from Amgen, GlaxoSmithKline and Sanofi and advisory role for GlaxoSmithKline; KM has received honoraria from Celgene, Takeda, Amgen, Sanofi and Janssen; LP has received honoraria from GlaxoSmithKline, Sanofi and Pfizer; PT has received honoraria from Amgen, Bristol-Myers Squibb/Celgene, Janssen, Takeda, AbbVie, Sanofi, GlaxoSmithKline and Pfizer; CN has received consultant honoraria from Keosys and funding from Radius, Immedica, Thema Sinergie; MC has served as Consulting/advisory role for and has received honoraria from Amgen, AbbVie, Bristol-Myers Squibb, Celgene, GlaxoSmithKline, Janssen, Menarini Stemline, Sanofi, and Karyopharm Therapeutics; EZ has received honoraria from Janssen, Bristol-Myers Squibb, Amgen, Takeda. MT, SB, AC, IS, EM, RR, SM, FB, MP, and MI declare no potential conflict of interest.

Author Contributions

MT designed the research study, performed bibliography research and analysis of published data, and wrote the original draft of the paper. SB collaborated on manuscript preparation, offered editorial support and critically revised the paper. AC, IS, EM, RR, SM, FB, MP, MI, IR, KM, LP, PT, CN helped in data collection and revised the paper. MC supervised the project and critically revised the paper. EZ conceived and supervised the research project, acquired fundings, discussed the results, and critically revised the paper. All authors discussed the results and contributed to the final version of the manuscript.

Funding

No funding was received for this work.

Institutional Review Board Statement

As this review uses information from previous literature, it does not require ethics approval and consent to participate.

Disclosures

I.Rizzello has received honoraria from Amgen, GlaxoSmithKline and Sanofi and advisory role for GlaxoSmithKline; K.Mancuso has received honoraria from Celgene, Takeda, Amgen, Sanofi and Janssen; L.Pantani has received honoraria from GlaxoSmithKline, Sanofi and Pfizer; P. Tacchetti has received honoraria from Amgen, Bristol-Myers Squibb/Celgene, Janssen, Takeda, AbbVie, Sanofi, GlaxoSmithKline and Pfizer; C.Nanni has received consultant honoraria from Keosys and funding from Radius, Immedica, Thema Sinergie; M.Cavo has served as Consulting/advisory role for and has received honoraria from Amgen, AbbVie, Bristol-Myers Squibb, Celgene, GlaxoSmithKline, Janssen, Menarini Stemline, Sanofi, and Karyopharm Therapeutics; E.Zamagni has received honoraria from Janssen, Bristol-Myers Squibb, Amgen, Takeda.

M.Talarico, S.Barbato, A.Cattabriga, I.Sacchetti, E.Manzato, R. Restuccia, S.Masci, F.Bigi, M.Puppi, and M.Iezza declare no potential conflict of interest.

References

[1] R.A. Kyle, M.A. Gertz, T.E. Witzig, et al., Review of 1027 patients with newly diagnosed multiple myeloma, *Mayo Clin. Proc.* 78 (1) (2003) 21–33.

[2] E. Terpos, J. Berenson, N. Raje, G.D. Roodman, Management of bone disease in multiple myeloma, *Expert Rev. Hematol.* 7 (1) (2014) 113–125.

[3] E. Terpos, J. Berenson, R.J. Cook, et al., Prognostic variables for survival and skeletal complications in patients with multiple myeloma osteolytic bone disease, *Leukemia* 24 (5) (2010) 1043–1049.

[4] L. Rosiñol, M. Beksac, E. Zamagni, et al., Expert review on soft-tissue plasmacytomas in multiple myeloma: definition, disease assessment and treatment considerations, *Br. J. Haematol.* 194 (3) (2021) 496–507.

[5] International Myeloma Working Group, Criteria for the classification of monoclonal gammopathies, multiple myeloma and related disorders: a report of the International Myeloma Working Group, *Br. J. Haematol.* 121 (5) (2003) 749–757.

[6] S.V. Rajkumar, M.A. Dimopoulos, A. Palumbo, et al., International Myeloma Working Group updated criteria for the diagnosis of multiple myeloma, *Lancet Oncol.* 15 (12) (2014) e538–e548.

[7] J. Hillengass, K. Fechtner, M.A. Weber, et al., Prognostic significance of focal lesions in whole-body magnetic resonance imaging in patients with asymptomatic multiple myeloma, *J. Clin. Oncol.* 28 (9) (2010) 1606–1610.

[8] E. Kastritis, L.A. Moulopoulos, E. Terpos, et al., The prognostic importance of the presence of more than one focal lesion in spine MRI of patients with asymptomatic (smoldering) multiple myeloma, *Leukemia* 28 (12) (2014) 2402–2403.

[9] J. Hillengass, L.A. Moulopoulos, S. Delorme, et al., Whole-body computed tomography versus conventional skeletal survey in patients with multiple myeloma: a study of the International Myeloma Working Group, *Blood Cancer J.* 7 (8) (2017) e599.

[10] J. Hillengass, S. Usmani, S.V. Rajkumar, et al., International myeloma working group consensus recommendations on imaging in monoclonal plasma cell disorders, *Lancet Oncol.* 20 (6) (2019) e302–e312.

[11] E. Zamagni, C. Nanni, F. Patriarca, et al., A prospective comparison of 18F-fluorodeoxyglucose positron emission tomography-computed tomography, magnetic resonance imaging and whole-body planar radiographs in the assessment of bone disease in newly diagnosed multiple myeloma, *Haematologica* 92 (1) (2007) 50–55.

[12] P. Moreau, M. Attal, D. Caillot, et al., Prospective Evaluation of Magnetic Resonance Imaging and [18F]Fluorodeoxyglucose Positron Emission Tomography-Computed Tomography at Diagnosis and Before Maintenance Therapy in Symptomatic Patients With Multiple Myeloma Included in the IFM/DFCI 2009 Trial, *J. Clin. Oncol.* 35 (25) (2017) 2911–2918.

[13] E. Zamagni, F. Patriarca, C. Nanni, et al., Prognostic relevance of 18-F FDG PET/CT in newly diagnosed multiple myeloma patients treated with up-front autologous transplantation, *Blood* 118 (23) (2011) 5989–5995.

[14] T.B. Bartel, J. Haessler, T.L. Brown, et al., F18-fluorodeoxyglucose positron emission tomography in the context of other imaging techniques and prognostic factors in multiple myeloma, *Blood* 114 (10) (2009) 2068–2076.

[15] R. Fonti, M. Larobina, S. Del Vecchio, et al., Metabolic tumor volume assessed by 18F-FDG PET/CT for the prediction of outcome in patients with multiple myeloma, *J. Nucl. Med.* 53 (12) (2012) 1829–1835.

[16] J.E. McDonald, M.M. Kessler, M.W. Gardner, et al., Assessment of Total Lesion Glycolysis by 18F FDG PET/CT Significantly Improves Prognostic Value of GEP and ISS in Myeloma, *Clin. Cancer Res.* 23 (8) (2016) 1981–1987.

[17] P. Spinnato, A. Bazzocchi, A. Brioli, et al., Contrast enhanced MRI and ^{18}F-FDG PET-CT in the assessment of multiple myeloma: a comparison of results in different phases of the disease, *Eur. J. Radiol.* 81 (12) (2012) 4013–4018.

[18] R. Walker, B. Barlogie, J. Haessler, et al., Magnetic resonance imaging in multiple myeloma: diagnostic and clinical implications, *J. Clin. Oncol.* 25 (9) (2007) 1121–1128.

[19] J.C. Regelink, M.C. Minnema, E. Terpos, et al., Comparison of modern and conventional imaging techniques in establishing multiple myeloma-related bone disease: a systematic review, *Br. J. Haematol.* 162 (1) (2013) 50–61.

[20] R. Fonti, B. Salvatore, M. Quarantelli, et al., 18F-FDG PET/CT, 99mTc-MIBI, and MRI in evaluation of patients with multiple myeloma, *J. Nucl. Med.* 49 (2) (2008) 195–200.

[21] S. Kumar, B. Paiva, K.C. Anderson, et al., International Myeloma Working Group consensus criteria for response and minimal residual disease assessment in multiple myeloma, *Lancet Oncol.* 17 (8) (2016) 328–346.

[22] S.Z. Usmani, A. Mitchell, S. Waheed, et al., Prognostic implications of serial 18-fluoro-deoxyglucose emission tomography in multiple myeloma treated with total therapy 3, *Blood* 121 (10) (2013) 1819–1823.

[23] E. Zamagni, C. Nanni, K. Mancuso, et al., PET/CT Improves the Definition of Complete Response and Allows to Detect Otherwise Unidentifiable Skeletal Progression in Multiple Myeloma, *Clin. Cancer Res.* 21 (19) (2015) 4384–4390.

[24] C. Charalampous, U. Goel, S.M. Broski, et al., Utility of PET/CT in assessing early treatment response in patients with newly diagnosed multiple myeloma, *Blood Adv.* 6 (9) (2022) 2763–2772.

[25] P. Moreau, S. Zweegman, A. Perrot, et al., Evaluation of the Prognostic Value of Positron Emission Tomography-Computed Tomography at Diagnosis and Follow-up in Transplant-Eligible Newly Diagnosed Multiple Myeloma Patients Treated in the Phase 3 Cassiopeia Study: Results of the Cassiopet Companion, *Blood* 134 (Supplement 1) (2019) 692.

[26] C. Nanni, A. Versari, S. Chauvie, et al., Interpretation criteria for FDG PET/CT in multiple myeloma (IMPeTUs): final results. IMPeTUs (Italian myeloma criteria for PET USe), *Eur. J. Nucl. Med. Mol. Imaging* 45 (5) (2018) 712–719.

[27] E. Zamagni, C. Nanni, L. Dozza, et al., Standardization of 18F-FDG-PET/CT According to Deauville Criteria for Metabolic Complete Response Definition in Newly Diagnosed Multiple Myeloma, *J. Clin. Oncol.* 39 (2) (2021) 116–125.

[28] E. Zamagni, S. Oliva, F. Gay, et al., Impact of minimal residual disease standardised assessment by FDG-PET/CT in transplant-eligible patients with newly diagnosed multiple myeloma enrolled in the imaging sub-study of the FORTE trial, *EClinicalMedicine.* 60 (2023) 102017.

[29] J. Hillengass, S. Ayyaz, K. Kilk, et al., Changes in magnetic resonance imaging before and after autologous stem cell transplantation correlate with response and survival in multiple myeloma, *Haematologica* 97 (11) (2012) 1757–1760.

[30] **Hounsfield GN.** Computed medical imaging. Nobel lecture, Decemberr 8, 1979. *Journal of Computer Assisted Tomography.* 1980, Vol. 4, 5, pp. 665-674.

[31] C.H. McCollough, S. Leng, L. Yu, J.G. Fletcher, Dual- and Multi-Energy CT: Principles, Technical Approaches, and Clinical Applications, *Radiology* 276 (3) (2015) 637–653.

[32] T.R. Johnson, Dual-energy CT: general principles, *Am. J. Roentgenol.* 1995 (5 Suppl) (2012) S3–S8.

[33] R. García-Figueiras, L. Oleaga, J. Broncano, et al., What to Expect (and What Not) from Dual-Energy CT Imaging Now and in the Future? *Journal of Imaging.* 10 (7) (2024) 154.

[34] V. Rodríguez-Laval, B. Lumbreras-Fernández, et al., Imaging of Multiple Myeloma: Present and Future, *J. Clin. Med.* 13 (1) (2024) 264.

[35] C. Thomas, C. Schabel, B. Krauss, et al., Dual-energy CT: virtual calcium subtraction for assessment of bone marrow involvement of the spine in multiple myeloma, *Am. J. Roentgenol.* 204 (3) (2015) W324–W331.

[36] S.C. Brandelik, S. Skornitzke, T. Mokry, et al., Quantitative and qualitative assessment of plasma cell dyscrasias in dual-layer spectral CT, *Eur. Radiol.* 31 (10) (2021) 7664–7673.

[37] A. Kosmala, A.M. Weng, A. Heidemeier, et al., Multiple Myeloma and Dual-Energy CT: Diagnostic Accuracy of Virtual Noncalcium Technique for Detection of Bone Marrow Infiltration of the Spine and Pelvis, *Radiology* 286 (1) (2018) 205–213.

[38] A. Kosmala, A.M. Weng, B. Krauss, et al., Dual-energy CT of the bone marrow in multiple myeloma: diagnostic accuracy for quantitative differentiation of infiltration patterns, *Eur. Radiol.* 28 (12) (2018) 5083–5090.

[39] **Brandelik SC, Skornitzke S, Mokry T et al.** Quantitative and qualitative assessment of plasma cell dyscrasias in dual-layer spectral CT. *European Radiology.* 2021, Vol. 31, 10, pp. 7664-7673.

[40] S. Werner, B. Krauss, M. Horger, Dual-Energy CT-Based Bone Marrow Imaging in Multiple Myeloma: Assessment of Focal Lesions in Relation to Disease Status and MRI Findings, *Acad. Radiol.* 29 (2) (2022) 245–254.

[41] P. Fervers, A. Glauner, R. Gertz, et al., Virtual calcium-suppression in dual energy computed tomography predicts metabolic activity of focal MM lesions as determined by fluorodeoxyglucose positron-emission-tomography, *Eur. J. Radiol.* 135 (2021) 109502.

[42] P. Fervers, E. Celik, G. Bratke, et al., Radiotherapy Response Assessment of Multiple Myeloma: A Dual-Energy CT Approach With Virtual Non-Calcium Images, *Front. Oncol.* 11 (2021) 734819.

[43] R. Gu, A. Amlani, U. Haberland, et al., Correlation between whole skeleton dual energy CT calcium-subtracted attenuation and bone marrow infiltration in multiple myeloma, *Eur. J. Radiol.* 149 (2022) 110223.

[44] C.P. Reinert, E. Krieg, M. Esser, et al., Role of computed tomography texture analysis using dual-energy-based bone marrow imaging for multiple myeloma characterization: comparison with histology and established serologic parameters, *Eur. Radiol.* 31 (4) (2021) 2357–2367.

[45] J. Chen, Z. Qiu, N. Jiang, et al., Detecting bone marrow infiltration in nonosteolytic multiple myeloma through separation of hydroxyapatite via the two-material decomposition technique in spectral computed tomography, *Quant. Imaging Med. Surg.* 14 (2024) 3.

[46] N. Jiang, Y. Xia, M. Luo, et al., Diagnosis of newly developed multiple myeloma without bone disease detectable on conventional computed tomography (CT) scan by using dual-energy CT, *Journal of Bone Oncology.* 48 (2024) 100636.

[47] J. Cook, K. Rajendran, A. Ferrero, et al., Photon Counting Detector Computed Tomography: A New Frontier of Myeloma Bone Disease Evaluation, *Acta Haematol.* 146 (5) (2023) 419–423.

[48] F.I. Baffour, N.R. Huber, A. Ferrero, et al., Photon-counting Detector CT with Deep Learning Noise Reduction to Detect Multiple Myeloma, *Radiology* 306 (1) (2023) 229–236.

[49] M.T. Winkelmann, F. Hagen, L. Le-Yannou, et al., Myeloma bone disease imaging on a 1st-generation clinical photon-counting detector CT vs. 2nd-generation dual-source dual-energy CT, *Eur. Radiol.* 33 (4) (2023) 2415–2425.

[50] M. Cavo, E. Terpos, C. Nanni, et al., Role of 18F-FDG PET/CT in the diagnosis and management of multiple myeloma and other plasma cell disorders: a consensus statement by the International Myeloma Working Group, *Lancet Oncol.* 18 (4) (2017) e206–e217.

[51] L. Rasche, E. Angtuaco, J.E. McDonald, et al., Low expression of hexokinase-2 is associated with false-negative FDG-positron emission tomography in multiple myeloma, *Blood* 130 (1) (2017) 30–34.

[52] L. Bao, Y. Lai, Y. Liu, et al., CXCR4 is a good survival prognostic indicator in multiple myeloma patients, *Leuk. Res.* 37 (9) (2013) 1083–1088.

[53] K. Philipp-Abbrederis, K. Herrmann, et al., In vivo molecular imaging of chemokine receptor CXCR4 expression in patients with advanced multiple myeloma, *EMBO Mol. Med.* 7 (4) (2015) 477–487.

[54] T.R. Ullah, The role of CXCR4 in multiple myeloma: Cells' journey from bone marrow to beyond, *Journal of Bone Oncology.* 17 (2019) 100253.

[55] **Lapa C, Schreder M, Schirbel A et al.** [68Ga]Pentixafor-PET/CT for imaging of chemokine receptor CXCR4 expression in multiple myeloma - Comparison to [18F]FDG and laboratory values. *Theranostics.* 2017, Vol. 7, 1, pp. 205-212.

[56] Q. Pan, X. Cao, Y. Luo, et al., Chemokine receptor-4 targeted PET/CT with 68Ga-Pentixafor in assessment of newly diagnosed multiple myeloma: comparison to 18F-FDG PET/CT, *Eur. J. Nucl. Med. Mol. Imaging* 47 (3) (2020) 537–546.

[57] A.S. Shekhawat, B. Singh, P. Malhotra, et al., Imaging CXCR4 receptors expression for staging multiple myeloma by using 68Ga-Pentixafor PET/CT: comparison with 18F-FDG PET/CT, *Br. J. Radiol.* 95 (1136) (2022) 20211272.

[58] S. Kuyumcu, E.G. Isik, T.O. Tiryaki, et al., Prognostic significance of 68Ga-Pentixafor PET/CT in multiple myeloma recurrence: a comparison to 18F-FDG PET/CT and laboratory results, *Ann. Nucl. Med.* 35 (10) (2021) 1147–1156.

[59] K. Herrmann, M. Schottelius, C. Lapa, et al., First-in-Human Experience of CXCR4-Directed Endoradiotherapy with 177Lu- and 90Y-Labeled Pentixather in Advanced-Stage Multiple Myeloma with Extensive Intra- and Extramedullary Disease, *J. Nucl. Med.* 57 (2) (2016) 248–251.

[60] C. Lapa, K. Herrmann, A. Schirbel, CXCR4-directed endoradiotherapy induces high response rates in extramedullary relapsed Multiple Myeloma, *Theranostics.* 7 (6) (2017) 1589–1597.

[61] S. Maurer, P. Herhaus, R. Lippenmeyer, et al., Side Effects of CXC-Chemokine Receptor 4-Directed Endoradiotherapy with Pentixather Before Hematopoietic Stem Cell Transplantation, *J. Nucl. Med.* 60 (10) (2019) 1399–1405.

[62] R. Minamimoto, Amino Acid and Proliferation PET/CT for the Diagnosis of Multiple Myeloma, *Front. Nucl. Med.* 1 (2022) 796357.

[63] A. Dankerl, P. Liebisch, G. Glatting, et al., *Radiology* 242 (2) (2007) 498–508.

[64] Y. Nakamoto, K. Kurihara, M. Nishizawa, et al., Clinical value of ^{11}C-methionine PET/CT in patients with plasma cell malignancy: comparison with ^{18}F-FDG PET/CT, *Eur. J. Nucl. Med. Mol. Imaging* 40 (5) (2013) 708–715.

[65] C. Lapa, S. Knop, M. Schreder, et al., 11C-Methionine-PET in Multiple Myeloma: Correlation with Clinical Parameters and Bone Marrow Involvement, *Theranostics.* 6 (2) (2016) 254–261.

[66] M.I. Morales-Lozano, P. Rodriguez-Otero, et al., 1C-Methionine PET/CT in Assessment of Multiple Myeloma Patients: Comparison to 18F-FDG PET/CT and Prognostic Value, *Int. J. Mol. Sci.* 23 (17) (2022) 9895.

[67] Y. Wang, A. Yee, Z. Bernstein, et al., Carbon-11-Labeled Methionine PET/CT in Patients With FDG-Occult Multiple Myeloma: A Prospective Pilot Study, *Am. J. Roentgenol.* 220 (2022) 4.

[68] S. Sagar, D. Khan, K.V. Sivasankar, R. Kumar, New PET Tracers for Symptomatic Myeloma, *PET Clinics.* 19 (4) (2024) 515–524.

[69] K. Lückerath, C. Lapa, A. Spahmann, et al., Targeting paraprotein biosynthesis for non-invasive characterization of myeloma biology, *PLoS One* 8 (12) (2013) e84840.

[70] C. Stokke, J.N. Nørgaard, H. Feiring Phillips, et al., Comparison of [18F] fluciclovine and [18F]FDG PET/CT in Newly Diagnosed Multiple Myeloma Patients, *Mol. Imag. Biol.* 24 (5) (2022) 842–851.

[71] C. Nanni, E. Zamagni, M. Cavo, et al., 11C-choline vs. 18F-FDG PET/CT in assessing bone involvement in patients with multiple myeloma, *World J. Surg. Oncol.* 5 (2007) 68.

[72] C. Lapa, M. Kircher, M. Da Via, et al., Comparison of 11C-Choline and 11C-Methionine PET/CT in Multiple Myeloma, *Clin. Nucl. Med.* 44 (8) (2019) 620–624.

[73] T. Cassou-Mounat, S. Balogova, V. Nataf, et al., 18F-fluorocholine versus 18F-fluorodeoxyglucose for PET/CT imaging in patients with suspected relapsing or progressive multiple myeloma: a pilot study, *Eur. J. Nucl. Med. Mol. Imaging* 43 (11) (2016) 1995–2004.

[74] P. Garrastachu Zumarán, I. García Megías, et al., Multitracer PET/CT with [18F] Fluorodeoxiglucose and [18F]Fluorocholine in the Initial Staging of Multiple Myeloma Patients Applying the IMPeTus Criteria: A Pilot Study, *Diagnostics (basel).* 13 (9) (2023) 1570.

[75] C.L. Ho, S. Chen, Y.L. Leung, et al., 11C-acetate PET/CT for metabolic characterization of multiple myeloma: a comparative study with 18F-FDG PET/CT, *J. Nucl. Med.* 55 (5) (2014) 749–752.

[76] **Lin C, Ho CL, Ng SH et al.** (11)C-acetate as a new biomarker for PET/CT in patients with multiple myeloma: initial staging and postinduction response assessment. *European Journal of Nuclear Medicine and Molecular Imaging.* 2014, Vol. 41, 1, pp. 41-49.

[77] M. Chen, W. Zhu, J. Du, et al., 11C-acetate positron emission tomography is more precise than 18F-fluorodeoxyglucose positron emission tomography in evaluating tumor burden and predicting disease risk of multiple myeloma, *Sci. Rep.* 11 (1) (2021) 22188.

[78] M. Okasaki, K. Kubota, R. Minamimoto, et al., Comparison of (11)C-4'-thiothymidine, (11)C-methionine, and (18)F-FDG PET/CT for the detection of active lesions of multiple myeloma, *Ann. Nucl. Med.* 29 (3) (2015) 224–232.

[79] C. Sachpekidis, H. Goldschmidt, K. Kopka, et al., Assessment of glucose metabolism and cellular proliferation in multiple myeloma: a first report on combined 18F-FDG and 18F-FLT PET/CT imaging, *EJNMMI Res.* 8 (1) (2018) 28.

[80] S.P.M. Souza, F.C. Frasson, M.E.S. Takahashi, et al., Head-to-head comparison of [68Ga]Ga-PSMA-11 and [18F]FDG PET/CT in multiple myeloma, *Eur. J. Nucl. Med. Mol. Imaging* 50 (8) (2023) 2432–2440.

[81] *EPS-205: Prospective Comparison of [18F]FDG and [68Ga]Ga-PSMA PET/CT in Staging Multiple Myeloma.* **Di Franco M, Bezzi D, Talarico M et al.** 2024. EANM.

[82] E.G. De Waal, R.H. Slart, M.J. Leene, et al., 18F-FDG PET increases visibility of bone lesions in relapsed multiple myeloma: is this hypoxia-driven? *Clin. Nucl. Med.* 40 (4) (2015) 291–296.

[83] C. Sachpekidis, H. Goldschmidt, D. Hose, et al., PET/CT studies of multiple myeloma using (18) F-FDG and (18) F-NaF: comparison of distribution patterns and tracers' pharmacokinetics, *Eur. J. Nucl. Med. Mol. Imaging* 41 (7) (2014) 1343–1353.

[84] C. Sachpekidis, J. Hillengass, H. Goldschmidt, et al., Treatment response evaluation with 18F-FDG PET/CT and 18F-NaF PET/CT in multiple myeloma patients undergoing high-dose chemotherapy and autologous stem cell transplantation, *Am. J. Nucl. Med. Mol. Imaging* 7 (4) (2017) 148–156.

[85] İ. Ak, H. Onner, O.M. Akay, Is there any complimentary role of F-18 NaF PET/CT in detecting of osseous involvement of multiple myeloma? A comparative study for F-18 FDG PET/CT and F-18 FDG NaF PET/CT, *Ann. Hematol.* 94 (9) (2015) 1567–1575.

[86] U. Elboga, E. Sahin, Y.B. Cayirli, et al., Comparison of [68Ga]-FAPI PET/CT and [18F]-FDG PET/CT in Multiple Myeloma: Clinical Experience, *Tomography.* 8 (1) (2022) 293–302.

[87] G.A. Ulaner, N.B. Sobol, J.A. O'Donoghue, et al., CD38-targeted Immuno-PET of Multiple Myeloma: From Xenograft Models to First-in-Human Imaging, *Radiology* 295 (3) (2020) 606–615.

[88] M.A. Dimopoulos, J. Hillengass, S. Usmani, et al., Role of magnetic resonance imaging in the management of patients with multiple myeloma: a consensus statement, *J. Clin. Oncol.* 33 (6) (2015) 657–664.

[89] S. Nosàs-Garcia, T. Moehler, K. Wasser, et al., Dynamic contrast-enhanced MRI for assessing the disease activity of multiple myeloma: a comparative study with histology and clinical markers, *J. Magn. Reson. Imaging* 22 (1) (2005) 154–162.

[90] J.C. Dutoit, K.L. Verstraete, MRI in multiple myeloma: a pictorial review of diagnostic and post-treatment findings, *Insights Imaging.* 7 (4) (2016) 553–569.

[91] V. Koutoulidis, N. Papanikolaou, L.A. Moulopoulos, Functional and molecular MRI of the bone marrow in multiple myeloma, *Br. J. Radiol.* 91 (1088) (2018) 20170389.

[92] J.C. Dutoit, M.A. Vanderkerken, K.L. Verstraete, Value of whole body MRI and dynamic contrast enhanced MRI in the diagnosis, follow-up and evaluation of disease activity and extent in multiple myeloma, *Eur. J. Radiol.* 82 (9) (2013) 1444–1452.

[93] B. Jamet, H. Necib, T. Carlier, et al., DCE-MRI to distinguish all monoclonal plasma cell disease stages and correlation with diffusion-weighted MRI/PET-based biomarkers in a hybrid simultaneous whole body-2-[18F]FDG-PET/MRI imaging approach, *Cancer Imaging* 24 (1) (2024) 93.

[94] J. Hillengass, J. Ritsch, M. Merz, et al., Increased microcirculation detected by dynamic contrast-enhanced magnetic resonance imaging is of prognostic significance in asymptomatic myeloma, *Br. J. Haematol.* 174 (1) (2016) 127–135.

[95] M. Merz, J. Ritsch, C. Kunz, et al., Dynamic contrast-enhanced magnetic resonance imaging for assessment of antiangiogenic treatment effects in multiple myeloma, *Clin. Cancer Res.* 21 (1) (2015) 106–112.

[96] J. Hillengass, K. Wasser, S. Delorme, et al., Lumbar bone marrow microcirculation measurements from dynamic contrast-enhanced magnetic resonance imaging is a predictor of event-free survival in progressive multiple myeloma, *Clin. Cancer Res.* 13 (2007) 2.

[97] M. Merz, T.M. Moehler, J. Ritsch, et al., Prognostic significance of increased bone marrow microcirculation in newly diagnosed multiple myeloma: results of a prospective DCE-MRI study, *Eur. Radiol.* 16 (5) (2016) 1404–1411.

[98] J.C. Dutoit, E. Claus, F. Offner, et al., Combined evaluation of conventional MRI, dynamic contrast-enhanced MRI and diffusion weighted imaging for response evaluation of patients with multiple myeloma, *Eur. J. Radiol.* 85 (2) (2016) 373–382.

[99] C. Lin, A. Luciani, K. Belhadj, et al., Multiple myeloma treatment response assessment with whole-body dynamic contrast-enhanced MR imaging, *Radiology* 254 (2) (2010) 521–531.

[100] T. Van Den Berghe, K.L. Verstraete, F.E. Lecouvet, et al., Review of diffusion-weighted imaging and dynamic contrast-enhanced MRI for multiple myeloma and its precursors (monoclonal gammopathy of undetermined significance and smouldering myeloma), *Skeletal Radiol.* 51 (1) (2022) 101–122.

[101] E.J. Bernstein, C. Schmidt-Lauber, J. Kay, Nephrogenic systemic fibrosis: a systemic fibrosing disease resulting from gadolinium exposure, *Best Pract. Res. Clin. Rheumatol.* 26 (4) (2012) 489–503.

[102] C. Messiou, J. Hillengass, S. Delorme, et al., Guidelines for Acquisition, Interpretation, and Reporting of Whole-Body MRI in Myeloma: Myeloma Response Assessment and Diagnosis System (MY-RADS), *Radiology* 291 (1) (2019) 5–13.

[103] J. Hillengass, T. Bäuerle, R. Bartl, et al., Diffusion-weighted imaging for non-invasive and quantitative monitoring of bone marrow infiltration in patients with monoclonal plasma cell disease: a comparative study with histology, *Br. J. Haematol.* 153 (6) (2011) 721–728.

[104] S.D. Almeida, J. Santinha, F.P.M. Oliveira, et al., Quantification of tumor burden in multiple myeloma by atlas-based semi-automatic segmentation of WB-DWI, *Cancer Imaging* 20 (1) (2020) 6.

[105] P. Torkian, B. Mansoori, J. Hillengass, et al., Diffusion-weighted imaging (DWI) in diagnosis, staging, and treatment response assessment of multiple myeloma: a systematic review and meta-analysis, *Skeletal Radiol.* 52 (3) (2023) 565–583.

[106] **Rasche L, Angtuaco E, McDonald JE et al.** Low expression of hexokinase-2 is associated with false-negative FDG-positron emission tomography in multiple myeloma. *Blood.* 2017, Vol. 130, 1, pp. 30-34.

[107] C. Mesguich, C. Hulin, V. Latrabe, et al., Prospective comparison of 18-FDG PET/CT and whole-body diffusion-weighted MRI in the assessment of multiple myeloma, *Ann. Hematol.* 99 (12) (2020) 2869–2880.

[108] J. Chen, C. Li, Y. Tian, et al., Comparison of Whole-Body DWI and 18F-FDG PET/CT for Detecting Intramedullary and Extramedullary Lesions in Multiple Myeloma, *Am. J. Roentgenol.* 213 (3) (2019) 514–523.

[109] C. Sachpekidis, J. Mosebach, M.T. Freitag, et al., Application of (18)F-FDG PET and diffusion weighted imaging (DWI) in multiple myeloma: comparison of

functional imaging modalities, *Am. J. Nucl. Med. Mol. Imaging* 5 (5) (2015) 479–492.
[110] O. Westerland, A. Amlani, C. Kelly-Morland, et al., Comparison of the diagnostic performance and impact on management of 18F-FDG PET/CT and whole-body MRI in multiple myeloma, *Eur. J. Nucl. Med. Mol. Imaging* 48 (8) (2021) 2558–2565.
[111] C. Messiou, N. Porta, B. Sharma, et al., Prospective Evaluation of Whole-Body MRI versus FDG PET/CT for Lesion Detection in Participants with Myeloma, *Radiol. Imaging Cancer* 3 (5) (2021) e210048.
[112] M. Talarico, G. De Cicco, P. Tacchetti, et al., Prospective Functional Bone Disease Evaluation of Newly Diagnosed Multiple Myeloma with Combined Use of (18)F-FDG-PET/CT and Whole-Body Diffusion Weighted Magnetic Resonance, *Clin. Lymphoma Myeloma Leuk.* 24 (Supplement 2) (2024) S10.
[113] L. Rasche, E.J. Angtuaco, T.L. Alpe, et al., The presence of large focal lesions is a strong independent prognostic factor in multiple myeloma, *Blood* 132 (1) (2018) 59–66.
[114] T. Terao, Y. Machida, K. Narita, et al., Total diffusion volume in MRI vs. total lesion glycolysis in PET/CT for tumor volume evaluation of multiple myeloma, *Eur. Radiol.* 31 (8) (2021) 6136–6144.
[115] C. Mesguich, V. Latrabe, C. Hulin, et al., Comparison of 18-FDG PET/CT and Whole-Body MRI with Diffusion-Weighted Imaging in the Evaluation of Treatment Response of Multiple Myeloma Patients Eligible for Autologous Stem Cell Transplant, *Cancers (Basel)* 13 (8) (2021) 1938.
[116] D. Costachescu, I. Ionita, E.C. Borsi, et al., Whole-body diffusion-weighted magnetic resonance imaging and apparent diffusion coefficient values as prognostic factors in multiple myeloma, *Exp. Ther. Med.* 22 (2) (2021) 827.
[117] B. Zhang, B. Bian, Y. Zhang, et al., The Apparent Diffusion Coefficient of Diffusion-Weighted Whole-Body Magnetic Resonance Imaging Affects the Survival of Multiple Myeloma Independently, *Front. Oncol.* 12 (2022) 780078.
[118] A. Latifoltojar, M. Hall-Craggs, N. Rabin, et al., Whole body magnetic resonance imaging in newly diagnosed multiple myeloma: early changes in lesional signal fat fraction predict disease response, *Br. J. Haematol.* 176 (2) (2017) 222–233.
[119] M. Takasu, S. Kondo, Y. Akiyama, et al., Assessment of early treatment response on MRI in multiple myeloma: Comparative study of whole-body diffusion-weighted and lumbar spinal MRI, *PLoS One* 15 (2) (2020) e0229607.
[120] S.L. Giles, C. Messiou, D.J. Collins, et al., Whole-body diffusion-weighted MR imaging for assessment of treatment response in myeloma, *Radiology* 271 (3) (2014) 785–794.
[121] C. Messiou, S. Giles, D.J. Collins, et al., Assessing response of myeloma bone disease with diffusion-weighted MRI, *Br. J. Radiol.* 85 (1020) (2012) e1198–e1203.
[122] C. Wu, J. Huang, W.B. Xu, et al., Discriminating Depth of Response to Therapy in Multiple Myeloma Using Whole-body Diffusion-weighted MRI with Apparent Diffusion Coefficient: Preliminary Results From a Single-center Study, *Acad. Radiol.* 25 (7) (2018) 904–914.
[123] K. Narita, Y. Machida, A. Kuzume, et al., Total Diffusion Volume Estimated By Whole-Body Diffusion Magnetic Resonance Imaging for the Assessment of Tumor Burden in Multiple Myeloma, *Blood* 136 (Supplement 1) (2020) 1.
[124] K. Narita, Y. Machida, D. Ikeda, et al., Total Diffusion Volume Evaluated By Whole-Body Diffusion Weighted Magnetic Resonance Image for the Assessment of Tumor Burden in Multiple Myeloma; Relations with Measurable Residual Disease Evaluated By Next-Generation Flow Cytometry and Bone Marrow CD138, *Blood* (2024).
[125] V. Koutoulidis, E. Terpos, N. Papanikolaou, et al., Comparison of MRI Features of Fat Fraction and ADC for Early Treatment Response Assessment in Participants with Multiple Myeloma, *Radiology* 304 (1) (2022) 137–144.
[126] L. Rasche, D. Alapat, M. Kumar, et al., Combination of flow cytometry and functional imaging for monitoring of residual disease in myeloma, *Leukemia* 33 (7) (2019) 1713–1722.
[127] A. Belotti, R. Ribolla, V. Cancelli, et al., Predictive role of diffusion-weighted whole-body MRI (DW-MRI) imaging response according to MY-RADS criteria after autologous stem cell transplantation in patients with multiple myeloma and combined evaluation with MRD assessment by flow cytometry, *Cancer Med.* 10 (17) (2021) 5859–5865.
[128] A. Belotti, R. Ribolla, C. Crippa, et al., Predictive role of sustained imaging MRD negativity assessed by diffusion-weighted whole-body MRI in multiple myeloma, *Am. J. Hematol.* 98 (9) (2023) e230–e232.
[129] S. Rama, C.H. Suh, K.W. Kim, et al., Comparative Performance of Whole-Body MRI and FDG PET/CT in Evaluation of Multiple Myeloma Treatment Response: Systematic Review and Meta-Analysis, *Am. J. Roentgenol.* 218 (4) (2022) 602–613.
[130] C. Schinke, L. Rasche, C. Ashby, et al., Sequential Imaging with Diffusion-Weighted Whole-Body MRI (DW-MRI) and PET-CT Identifies Patients at High Risk of Relapse in Multiple Myeloma, *Blood* 142 (Supplement 1) (2023) 882.
[131] **National Institute for Health and Care Excellence.** Myeloma: diagnosis and management. *NICE guideline [NG35]*. [Online] 2018. https://www.nice.org.uk/guidance/ng35/chapter/Recommendations#imaging-investigations.
[132] A. Chantry, M. Kazmi, S. Barrington, et al., Guidelines for the use of imaging in the management of patients with myeloma, *Br. J. Haematol.* 178 (3) (2017) 380–393.
[133] C. Sachpekidis, J. Hillengass, H. Goldschmidt, et al., Comparison of (18)F-FDG PET/CT and PET/MRI in patients with multiple myeloma, *Am. J. Nucl. Med. Mol. Imaging* 5 (5) (2015) 469–478.
[134] R. Burns, S. Mulé, P. Blanc-Durand, et al., Optimization of whole-body 2-[18F] FDG-PET/MRI imaging protocol for the initial staging of patients with myeloma, *Eur. Radiol.* 32 (5) (2022) 3085–3096.
[135] B. Jamet, T. Carlier, C. Bailly, et al., Hybrid simultaneous whole-body 2-[18F] FDG-PET/MRI imaging in newly diagnosed multiple myeloma: first diagnostic performance and clinical added value results, *Eur. Radiol.* 33 (9) (2023) 6438–6447.
[136] G. Barilà, F. Crimì, M. Arangio Febbo, et al., Imaging minimal residual disease evaluation in multiple myeloma using [18F]FDG PET/MRI, *Leuk. Lymphoma* 64 (2) (2023) 503–506.
[137] A.G. Ormond Filho, B.C. Carneiro, D. Pastore, et al., Whole-Body Imaging of Multiple Myeloma: Diagnostic Criteria, *Radiographics* 39 (4) (2019) 1077–1097.